Supplemental Materials for:

The Effects of High Angular Momentum on the Unimolecular Dissociation of CD_2CD_2OH: Theory and Comparisons with Experiment

Benjamin G. McKown[1], Michele Ceriotti[2], Caroline C. Womack[1], Eugene Kamarchik[3], Laurie J. Butler[*,1], and Joel M. Bowman[4]*

[1] Department of Chemistry and the James Franck Institute, University of Chicago, Chicago, Illinois 60637, USA

[2] Institute of Materials, École Polytechnique Fédérale de Lausanne (EPFL), CH-1015 Lausanne, Switzerland

[3] Combustion Research Facility, Sandia National Laboratories, Livermore, California 94551, USA

[4] Cherry L. Emerson Center for Scientific Computation, Department of Chemistry, Emory University, Atlanta, Georgia 30322, USA

Sketch Map

High-dimensional description of CD_2CD_2OH

A preliminary step for applying sketch map is the definition of a high-dimensional description of the system that captures the physics of the problem and removes details that are clearly unnecessary. For instance, the high-dimensional description should not depend on the orientation of the molecule in Cartesian coordinates, and should not differentiate between configurations in which the fragments are at different distances from each other, beyond a threshold at which they can be identified as separate chemical entities.

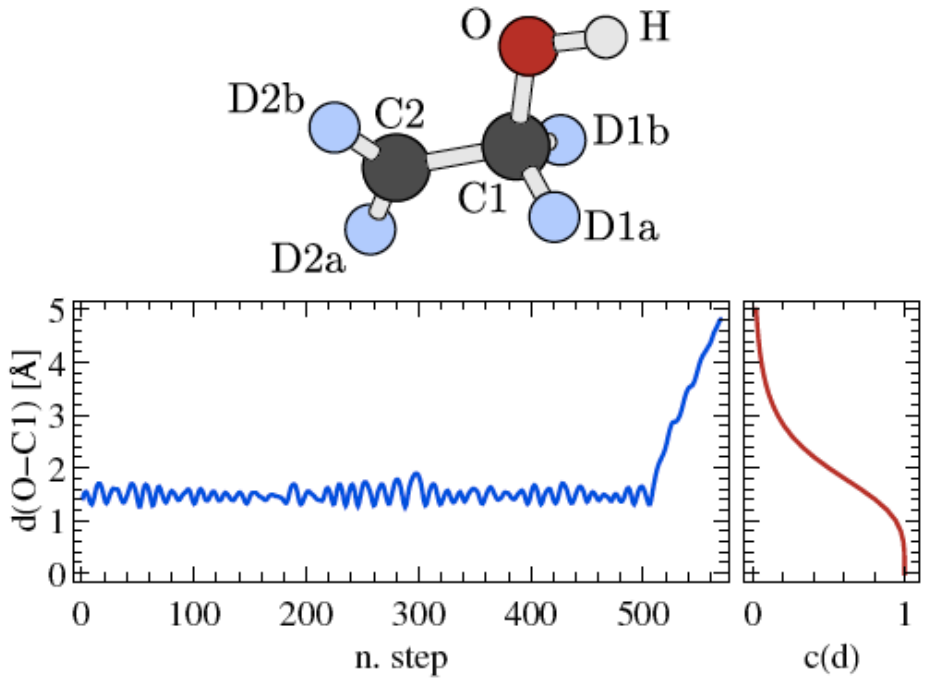

Figure 1: We chose 10 parameters to describe the configuration of CD_2CD_2OH and of its fragments. These collective variables are built using a bond-counting function $c(d)$ applied to different inter-atomic distances. The exponent a in this function was set to 4, which guarantees that $c(d)$ tapers off smoothly towards zero. The cutoff distance d_0 was chosen by observing the typical fluctuations in the intact CD_2CD_2OH, so as to discriminate between intact and broken bonds. With reference to the labels given in the figure above, we used the collective variables: 1) $c(d(\mathrm{C1}-\mathrm{C2}))$ ($d_0 = 1.80$ Å); 2) $c(d(\mathrm{O}-\mathrm{H}))$ ($d_0 = 1.20$ Å); 3) $c(d(\mathrm{O}-\mathrm{C1}))$ ($d_0 = 2.00$ Å); 4) $c(d(\mathrm{O}-\mathrm{C2}))$ ($d_0 = 2.00$ Å); 5) $c(d(\mathrm{H}-\mathrm{C1}))$ ($d_0 = 3.00$ Å); 6) $c(d(\mathrm{H}-\mathrm{C2}))$ ($d_0 = 4.00$ Å); 7) $c(d(\mathrm{O}-\mathrm{D1a}))+c(d(\mathrm{O}-\mathrm{D1b}))$ ($d_0 = 2.50$ Å); 8) $c(d(\mathrm{O}-\mathrm{D2a}))+c(d(\mathrm{O}-\mathrm{D2b}))$ ($d_0 = 2.50$ Å); 9) $c(d(\mathrm{C1}-\mathrm{D1a})) + c(d(\mathrm{C1}-\mathrm{D1b}))$ ($d_0 = 1.50$ Å); 10) $c(d(\mathrm{C2}-\mathrm{D2a})) + c(d(\mathrm{C2}-\mathrm{D2b}))$ ($d_0 = 1.50$ Å).

To address the first requirement, one can simply use a set of particle-particle distances to describe the geometry of the system. To address the second, one can transform these distances with a smooth step function, that effectively counts the number of existing bonds $c(d) = [1 + (d/d_0)^a]^{-1}$. The threshold distance

d_0 can be set by looking at the typical fluctuations in the intact molecule, as discussed in the caption of Figure 1.

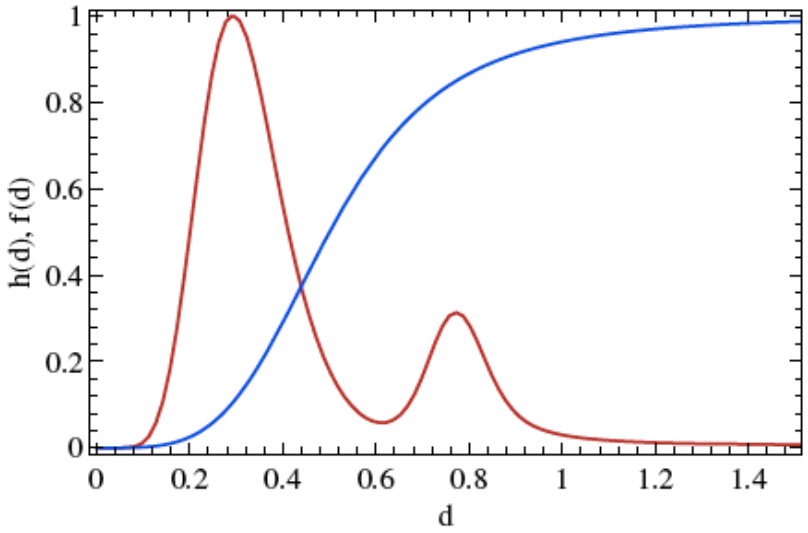

Figure 2: Histogram of distances between the 10-dimensional vectors describing several configurations of the CD_2CD_2OH encountered along 20 reactive trajectories. One can clearly identify one peak that correspond to fluctuations that do not lead to break-up of the original molecule, and one that corresponds to fragments. An effective sketch-map sigmoid function should transform to near zero distances that correspond to these short-range fluctuations. The function depicted in blue corresponds to the values $\sigma = 0.5$, $a = b = 4$ that have been used in this study.

Having defined in this way 10 collective variables that describe thoroughly the atomic configurations corresponding to the possible dissociation events, one can proceed to select representative snapshots from a set of reactive trajectories. We used a min-max criterion to select 250 landmarks, and proceeded to apply sketch-map to find an effective low-dimensional representation. The choice of the map parameters can be made by considering the range of distances between the points in the high-dimensional representation. As explained in Figure 2, one can clearly detect a range of distances that correspond to local, non-reactive fluctuations that should be ignored. A set of parameters that can filter reactive events from thermal fluctuations is $\sigma = 0.5$, $a = b = 4$. The resulting map can clearly describe the portion of the potential energy surface accessible at the energies considered in this study, as discussed in the main text.

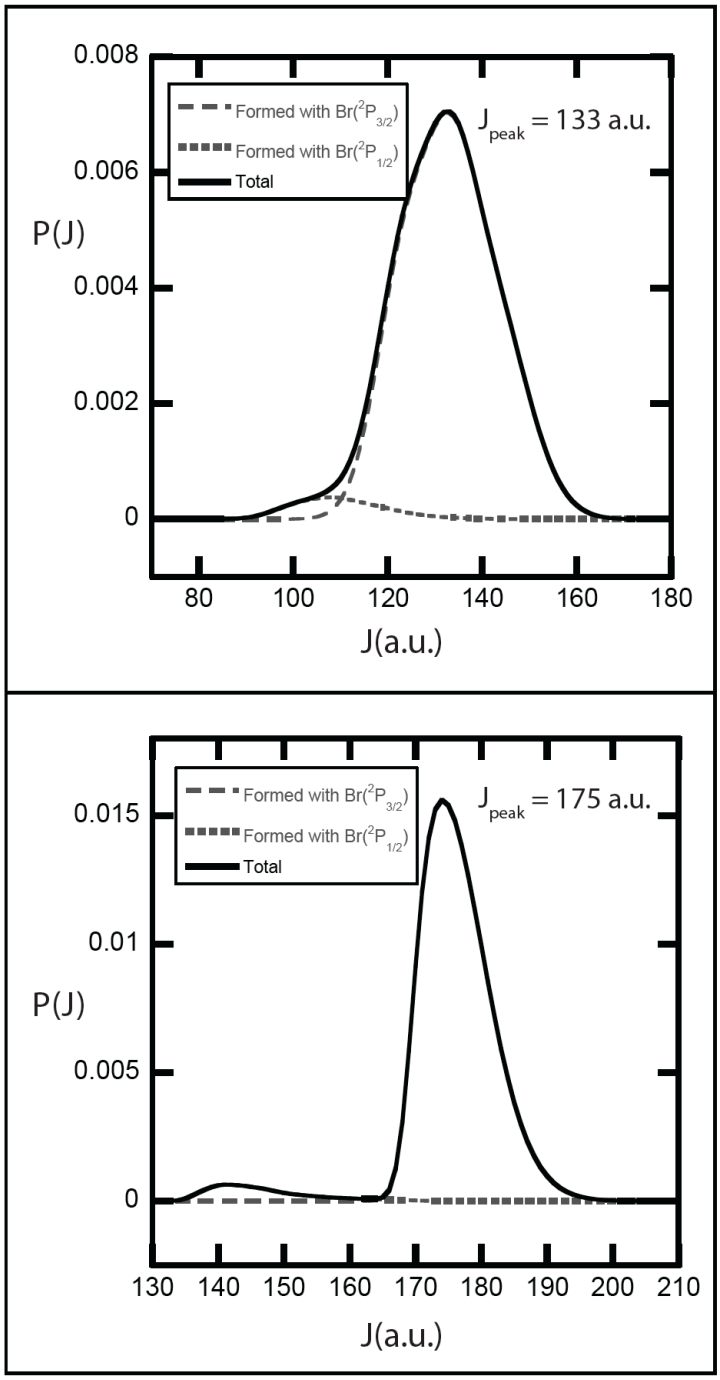

Figure 3: Representative slices from the distributions plotted in the middle and bottom frames of Figure 1 in the manuscript. The top frame here shows the distribution of J's imparted to the radicals when the Tt conformer dissociates to produce radicals with an internal energy of E_{int}=48 kcal/mol (For radicals in coincidence with $Br(^2P_{3/2})$, the corresponding E_T to this E_{int} would be near 32 kcal/mol, depending on the internal energy in the precursor.) The bottom frame shows the distribution of J's imparted to the radicals when the Gg conformer dissociates to produce radicals with an internal energy of 46 kcal/mol. The slices here distinguish the radicals formed in conjunction with $Br(^2P_{3/2})$ vs. $Br(^2P_{1/2})$.

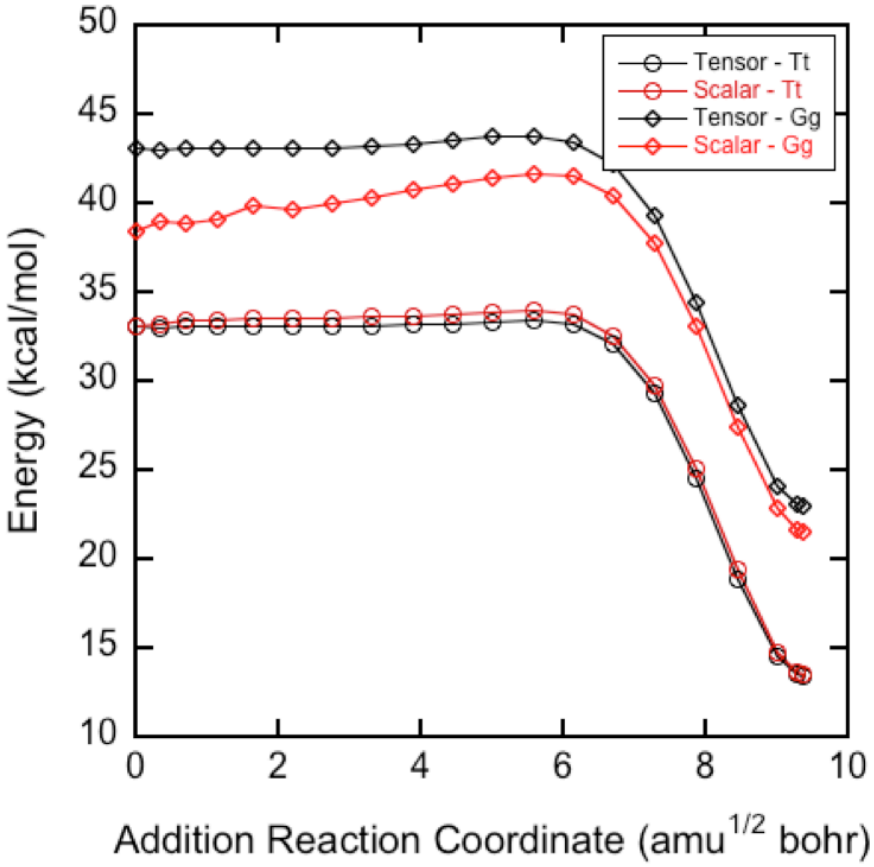

Figure 4: A comparison of the correct treatment of rotational energy in calculating an effective potential, versus a simple approximate treatment that is only correct if J is aligned with a principle axis of the molecule, so the tensor of inertia may be written as the one corresponding scalar component. The approximate treatment shown in red in the figure, uses $E_{rot} = \frac{1}{2} I \omega^2 = J^2/2I$ where I is the scalar diagonal element of the inertia tensor. The black lines show the correct treatment defined in the text and shown in blue line for the OH + ethene IRC in Figure 2 of the published manuscript. For CD_2CD_2OH radicals produced rotationally excited by photodissociating the Tt conformer of the precursor, J is nearly aligned with a principle axis of the molecule so either treatment may be used, but for radicals produced from photodissociating the Gg conformer the correct treatment should be used.

In Figure 8 of the published manuscript we use for the geometries sixteen images from a nudged-elastic-band calculation performed at the BLYP level of theory, starting from configurations taken from one of the trajectories yielding HOD+$CDCD_2$. The optimization of the IRC was interrupted before complete convergence, to obtain a near-minimum-energy-path that resembles the initial trajectory: the potential energy surface is very flat, and so further optimization would have changed very little the energy along the path, but led to large distortions in the geometry, with the OD fragment getting away from the ethene before turning back to abstract one D. The geometries corresponding to the images 1 through 16 on the x axis of Figure 8 (given below) were then used as input geometries for the comparison of the B3LYP single point energies and energies on the fitted potential energy surface used in the trajectory studies.

8

D	-0.0072135118	0.5622468538	1.2709825440
D	-0.4069640002	-1.1348015042	0.8904565251
D	1.5162354844	0.3651813099	-1.0392728321
D	1.9689694808	-1.0517890582	0.1199493997
H	-1.8512386307	0.6118207292	-0.0306689266
C	-0.0868739288	-0.1745119368	0.4383123242
C	1.2352034950	-0.3291772463	-0.2447346244
O	-1.0745026728	0.2984421186	-0.5359670937

8

D	-0.0677136270	0.6961573931	1.1279101316
D	-0.3300429120	-1.0738176474	1.0353990292
D	1.6080542945	0.4428564825	-0.9085546929
D	1.8593103992	-1.2300647395	-0.0878879293
H	-1.9446592062	0.2225946470	-0.1445418671
C	-0.0839556446	-0.1757029027	0.4389274841
C	1.2533547567	-0.3314642685	-0.2236261162
O	-1.0977494492	0.0468076109	-0.6041683951

8

D	-0.0929445523	0.7780888010	0.9503666618
D	-0.1766766641	-1.0289838512	1.1711123228
D	1.7462087553	0.4561144056	-0.7730672116
D	1.8167288881	-1.3469305725	-0.2891749056
H	-2.0671813003	-0.1379977175	-0.3709372623
C	0.0348970999	-0.1903891080	0.4744838413
C	1.3182965864	-0.3737526815	-0.2099985198
O	-1.1902423587	0.1216964715	-0.7479013878

8

D	-0.1517779871	0.7262213769	0.8672256512
D	-0.0415093836	-1.0865853658	1.3109501967

D	1.7142678835	0.4379400915	-0.7697855931
D	1.8653327226	-1.3573739548	-0.2915712323
H	-2.1887188448	-0.1280710312	-0.4386224050
C	0.3137330327	-0.2462565772	0.7065099397
C	1.3545807767	-0.3979112199	-0.1644042854
O	-1.5173335797	0.3199952202	-1.0108702871

8

D	-0.2653345244	0.5446567201	0.6187351729
D	0.1142193659	-1.1454336642	1.3284980886
D	1.6922083830	0.3431166115	-0.9157224436
D	2.1381964668	-1.2970054793	-0.1464161255
H	-2.3722441965	-0.0632083396	-0.5345966778
C	0.3733904809	-0.3453525377	0.6276562839
C	1.4570657383	-0.4412708958	-0.1911238918
O	-1.7027260771	0.5650595266	-0.9073169593

8

D	-0.4555387296	0.3136281030	0.3722134308
D	0.1331897530	-1.1839323483	1.3409971569
D	1.6297301379	0.2754304083	-0.9884647097
D	2.2990967494	-1.1266059972	0.0473578165
H	-2.4330606127	0.1147924177	-0.5259115251
C	0.3331312931	-0.4496130177	0.5537306019
C	1.4769363961	-0.4365269632	-0.1725684540
O	-1.7909006283	0.8566436698	-0.6583071280

8

D	-0.5491025291	0.1841694613	0.1753232366
D	0.0876802156	-1.1658106411	1.3140652162
D	1.6408615649	0.2392990814	-1.0187454258
D	2.3262671326	-1.0556228063	0.1378477218
H	-2.4947273384	0.4622357430	-0.5582832141
C	0.2920143658	-0.4993899968	0.4697053748
C	1.4767978154	-0.4362566696	-0.1739127656
O	-1.8582444373	1.1633518758	-0.2677257858

8

D	-0.6249021315	-0.0911600939	-0.0534389135
D	0.0873634355	-1.1852905627	1.2833993752
D	1.6434375395	0.1789770627	-1.0616685871
D	2.3627494494	-0.9427573521	0.2410057839
H	-2.7821262973	0.5844839971	-0.4805462760
C	0.2564141945	-0.5904128273	0.3807881531

C	1.4813641973	-0.4398424129	-0.1746132498
O	-2.1978213382	1.2675378781	-0.0622329672

8

D	-0.7110485873	0.2091010060	0.0746198491
D	-0.0334078456	-1.1152820650	1.2608634227
D	1.5942525132	0.2391263268	-1.0803397265
D	2.2617671530	-0.9540395524	0.1902179988
H	-2.4503371958	0.5484631307	-0.3980690470
C	0.2027072616	-0.5031937288	0.3856206215
C	1.4039709745	-0.3971145453	-0.2106247019
O	-1.7533561500	1.0998032045	0.0319976241

8

D	-1.0619794289	0.4453909137	-0.0279539701
D	0.0620825031	-1.2160579240	1.3701211730
D	1.6244620229	0.1693256009	-1.0492594360
D	2.4724338723	-0.9667599305	0.1710801343
H	-2.5341056394	0.3910759066	-0.5275157356
C	0.4032245377	-0.6676854233	0.4919994058
C	1.5457563715	-0.4749863007	-0.1657079907
O	-1.8592261994	1.0180694245	-0.2002659079

8

D	-1.0041128998	0.6095854745	-0.1297579301
D	0.2574012499	-1.1960904757	1.4421456158
D	1.8100582022	0.2434419165	-0.9496944358
D	2.5393962844	-1.2208945738	-0.0455625956
H	-2.4603807611	0.3117479343	-0.5544777984
C	0.6224368215	-0.5866523637	0.6143479494
C	1.7022614661	-0.5129474851	-0.1633475756
O	-1.7886131419	1.0223218547	-0.5632922506

8

D	-0.9629257410	0.6100068784	0.0201514081
D	0.3552897956	-1.2355514137	1.6342205649
D	1.8204245248	0.3639232520	-0.7077512808
D	2.3204324583	-1.3771884004	-0.2479386472
H	-2.4343822530	0.3621507593	-0.3754580299
C	0.7087618954	-0.5469653606	0.8680482125
C	1.6556378373	-0.5159425324	-0.0763288579
O	-1.7913169327	1.0836465253	-0.2234735569

8

D	-0.9691328619	0.4093476861	-0.3531283343
D	0.2497102274	-1.2340283548	1.4956617197
D	1.9135322906	0.3945376343	-0.6872374684
D	2.3357861236	-1.3734946204	-0.2473830350
H	-2.5047047671	0.3130763828	-0.2665434476
C	0.6722327951	-0.5294486894	0.7778010592
C	1.6864587976	-0.4958594947	-0.0882590746
O	-1.7910682415	0.8760864661	-0.6293814750

8

D	-0.9409208616	0.4169891297	-0.4499835392
D	0.2815746844	-1.2369217283	1.6046849734
D	1.9273948556	0.4492252133	-0.5489090358
D	2.0155366195	-1.4143930272	-0.4820849018
H	-2.4662977438	0.1992802151	-0.4698706679
C	0.7395798209	-0.4918020799	0.9519621110
C	1.6007673914	-0.4805557575	-0.0674944189
O	-1.7630626978	0.7401256183	-0.8802083863

8

D	-1.0179022676	0.4760403648	-0.4681924751
D	0.2961147093	-1.2050366992	1.6547801894
D	1.8769528905	0.5173312585	-0.5211144818
D	1.6939632127	-1.3327652246	-0.6831554793
H	-2.4482465717	-0.0215013119	-0.7550665245
C	0.7819439370	-0.4533362561	1.0309618962
C	1.4790093688	-0.4174438985	-0.1069157181
O	-1.8549355732	0.7402298727	-0.9070410108

8

D	-1.0787909213	0.3510950363	-0.4356434967
D	0.5442924806	-1.3162001330	1.7695923359
D	1.6372242952	0.5420077352	-0.5856468456
D	1.5274695944	-1.3118411347	-0.7737914528
H	-2.4446107499	-0.0517314925	-1.0299502570
C	0.8723102777	-0.5234648066	1.0954397099
C	1.3648508946	-0.4232371006	-0.1413106519
O	-1.8267317606	0.7027865011	-0.9640999420

Trajectory and Experimental Evidence for an HD + vinoxy-d_3 products

An unexpected result from the trajectories simulations showed the production of a partially deuterated hydrogen molecule and vinoxy radical. This product channel was initially discarded under the assumption that zero-point energy constraints were violated, as no such product channel appears on the PES of Senosiain et al.[12] or Womack et al.[18] A concerted HD loss transition state search starting from both the hydroxyl carbon and the radical carbon was undertaken with no such critical point able to be located at B3LPY/6-311++G(3dp,2pd). However, an HD loss transition state corresponding to a bimolecular collision between D and CD_2CDOH was found to be approximately 39 kcal mol^{-1} above the zero-point level of the CD_2CD_2OH radical, well within our experimental parameters. The eigenvector associated with the imaginary frequency revealed that the deuterium atom abstracts the hydrogen atom from ethenol to form vinoxy and HD. The calculated zero point corrected energy of the HD + vinoxy product channel is 9 kcal mol^{-1} above the CD_2CD_2OH radical intermediate.

Although this product channel has very modest branching, several trajectories were identified as dissociating into these products. These showed that one of the two C-D bonds on the hydroxyl carbon begins to elongate en route to forming ethenol + D (Figure 5, top frame). The deuterium atom then stays on a rather flat part of the PES allowing the two fragments to sample many relative configurations until the two dissociate completely, rejoin, or find an additional low energy pathway. For HD formation, a low energy pathway similar to a bimolecular collision between deuterium and ethenol is followed, rapidly forming vinoxy-d_3 + HD. In order to confirm this hypothesis, the potential energy and several interatomic distances were calculated and plotted for each molecular configuration of the trajectory. As can be seen in Figure 5 below, the potential energy stays roughly constant for a long period of time (tens to hundreds of femtoseconds) while the C-D and D-H distances remain large. Upon dissociation, the potential drops rapidly[†] and the H-D bond shortens.

[†] The potential decreases too much to be physically reasonably for this process. This is due to the insufficiency of the calculated potential surface for these given molecular configurations most likely caused by the pathway not being known prior to this investigation. Therefore, geometries corresponding to HD loss are poorly sampled for our fitted PES.

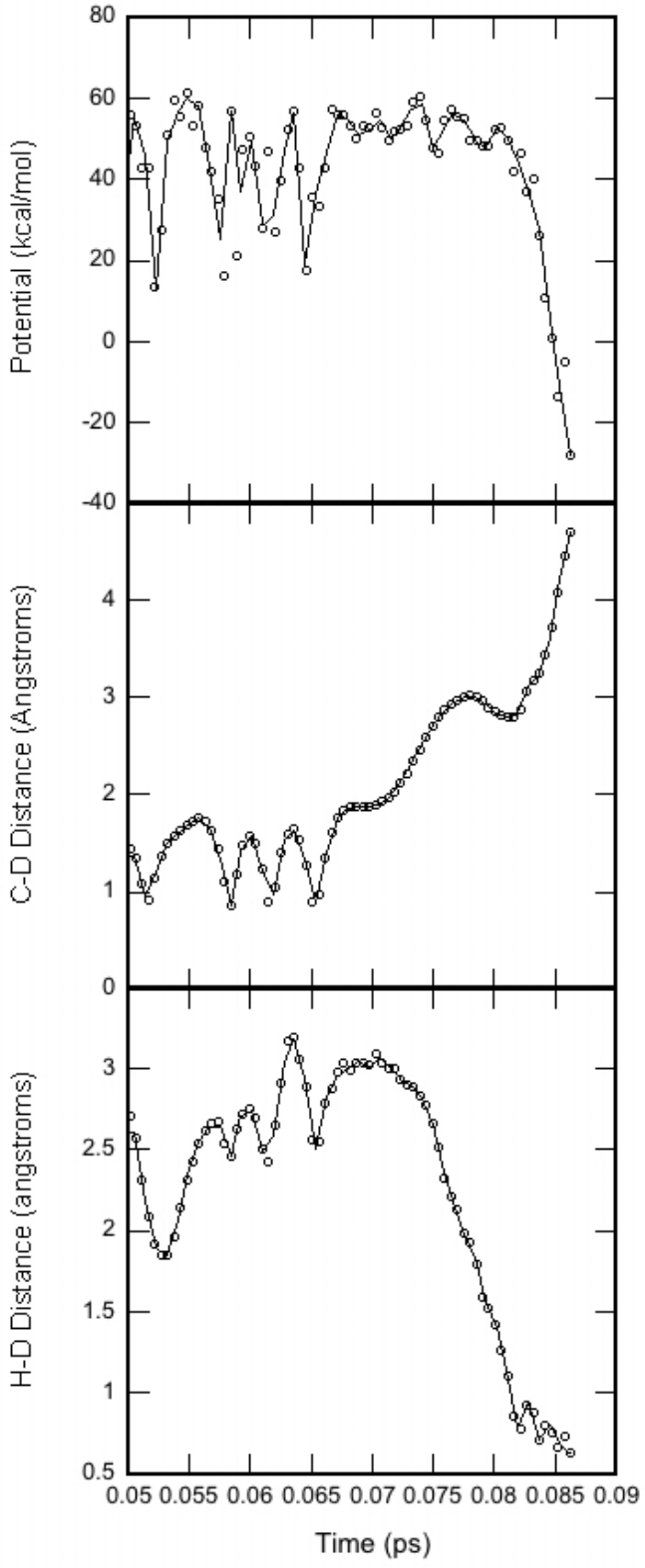

Figure 5: For a given HD "roaming" trajectory, the potential energy, carbon to leaving deuterium distance, and deuterium to hydrogen distance were plotted against time. As one can clearly see, the molecule experiences a flat portion of the potential while the C-D bond elongates. Following, the potential decreases greatly as the H-D distance shortens.

In our experimental study of this system,[19] we measured the recoil velocity of the Br and CH_2CD_2OH photofragments formed in the photodissociation of $BrCD_2CD_2OH$ so that the subsequent unimolecular dissociation dynamics of CD_2CD_2OH can be studied. The fragments were detected with tunable photoionization from a synchrotron at the National Synchrotron Radiation Research Center (NSRRC) in Hsinchu, Taiwan. The details of this crossed laser-molecular beam experiment are described in great detail in that paper. Reference 19 reports the fitted TOF spectra and the corresponding $P(E_T)$ for the primary photodissociation of $BrCD_2CD_2OH$ to form the Br and CD_2CD_2OH fragments. During that study, we also detected many of the secondary products of excited CD_2CD_2OH radicals which had sufficient energy to undergo subsequent dissociation. The major dissociation channels were found to be OH + ethene, HDO + C_2D_3 and CD_2H + CD_2O (the contribution from D + ethenol was obscured by an HBr primary photoelimination channel). We also detected a small amount of signal at a mass-to-charge ratio of 3 which we did not assign, but with the trajectory results described above we now attribute the m/e=3 signal to the HD of a minor vinoxy + HD product channel. While there is no direct dissociation pathway leading from CD_2CD_2OH to this exit channel, our trajectory calculations confirm that a small percentage of the excited radicals undergo a frustrated dissociation-like pathway leading to these products. Figure 6 below shows the TOF spectrum taken at m/e = 3, with the experimental data shown in red open circles and the fits shown in solid line. The data fit by the blue trace is attributed to dissociative ionization of stable CD_2CD_2OH radicals, and the remainder of the data is fit to the green trace, which was derived from the $P(E_T)$ shown in Figure 7 below with a $1/\sin(\theta)$ angular distribution. The vinoxy-d_3 co-fragment could not be definitively detected, but for completeness we show the m/e = 46 TOF spectrum fit with a contribution from a broad underlying signal from the proposed HD dissociation in Figure 8 below. The majority of the signal at m/e=46 is attributed to dissociative ionization of CD_2CD_2OH radicals (shown in blue), with some of the slower signal attributed to dissociative ionization of the CD_2CDOH co-fragment formed in a minor DBr photoelimination channel (orange). The remainder of the signal, fit in green, could be attributed to the roaming-type dissociation of excited radicals to HD + vinoxy, derived from the $P(E_T)$ shown in Figure 7. Both the m/e = 3 and m/e = 46 TOF spectra were fit assuming a $1/\sin(\theta)$ angular distribution. The low signal-to-noise of these spectra as well as the overlap of the various fits precludes any absolute certainty about the presence of these species, but the combination of the TOF plots and the trajectory

calculations is a good indication that HD + vinoxy may be a minor channel in the dissociation of CD_2CD_2OH.

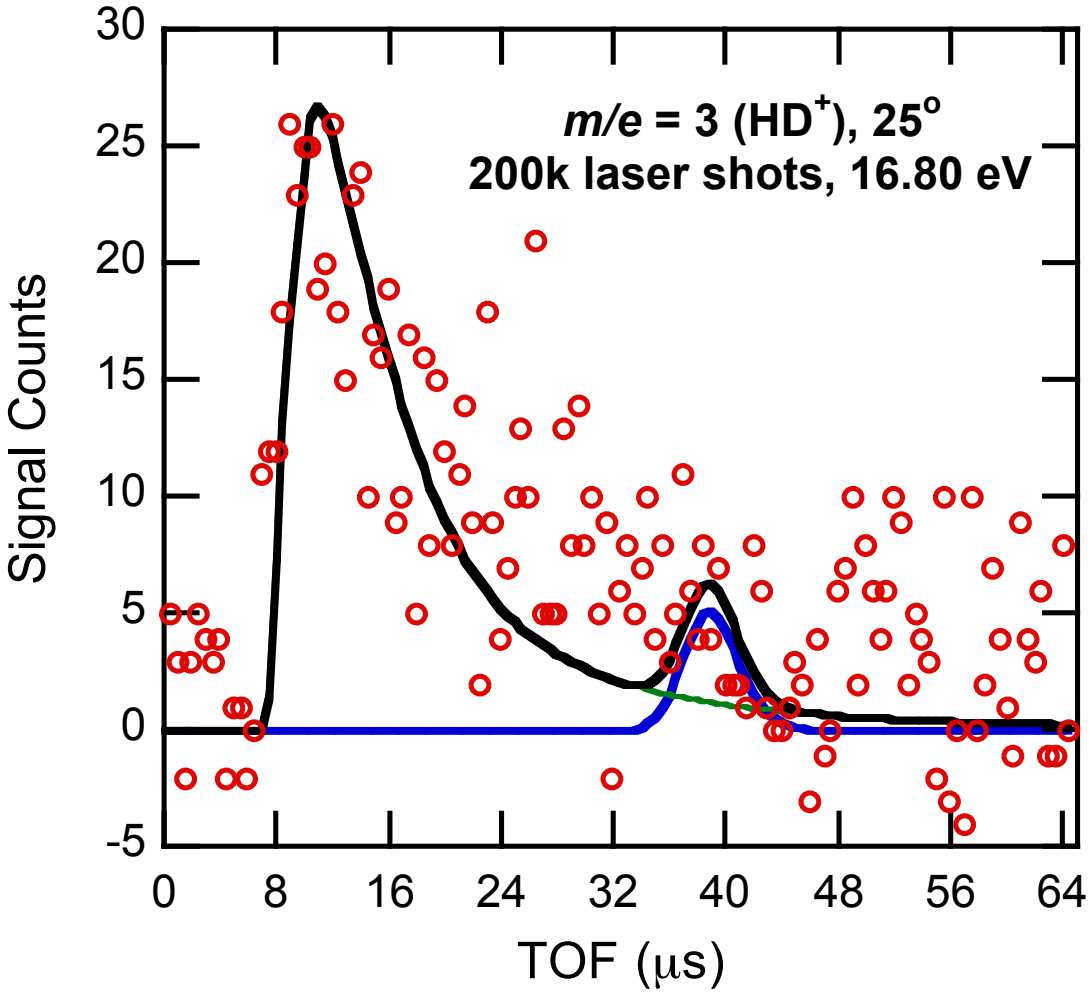

Figure 6: The time-of-flight (TOF) spectrum taken at m/e = 3 (HD^+). Data are shown in open circles, and the solid lines indicate forward convolution fits. The total fit is shown in black solid line and has contributions from the dissociative ionization of stable CD_2CD_2OH radicals (blue) and the dissociation pathway of unstable radicals to HD + vinoxy (green). The $P(E_T)$ used to derive this fit is shown in Figure 7 of this supplementary document.

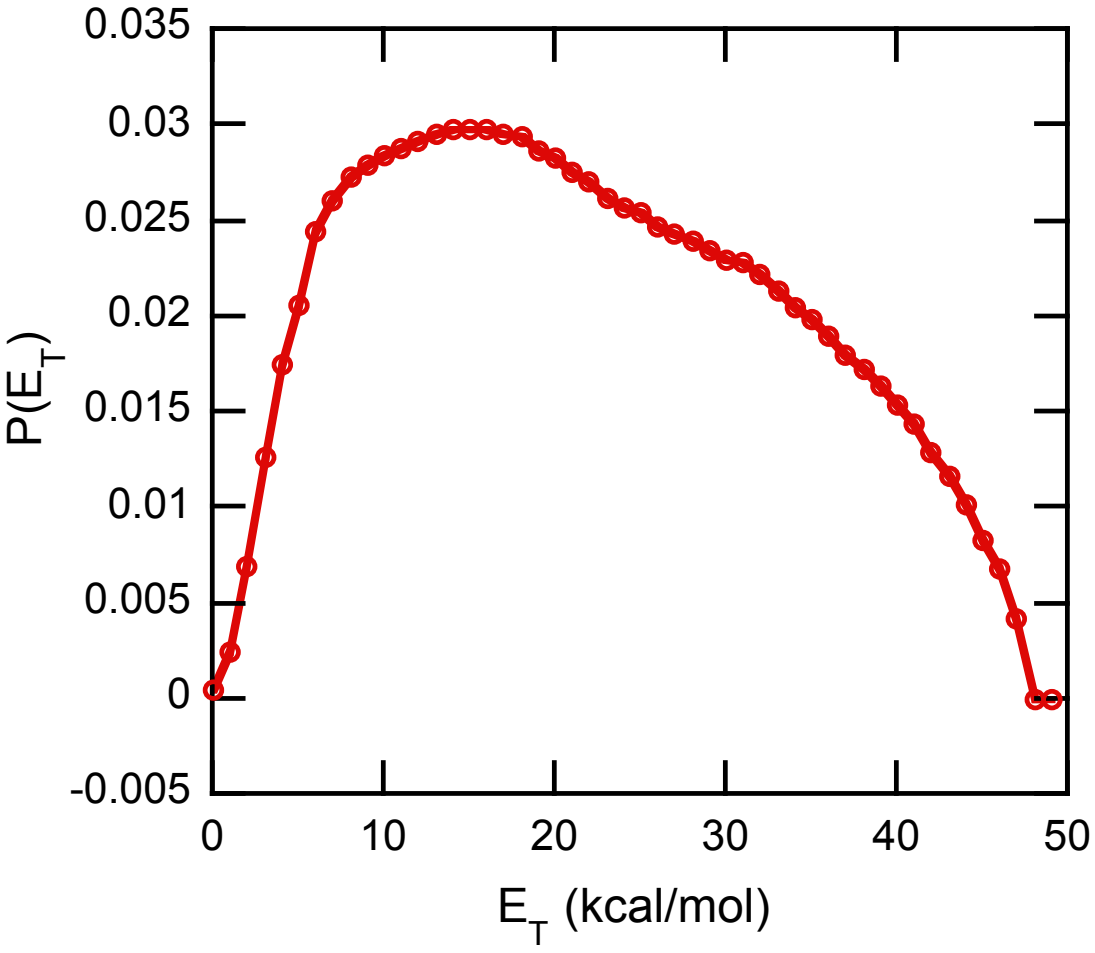

Figure 7: The center-of-mass translational energy distribution imparted to the HD and vinoxy fragments. This distribution was derived from the forward convolution fitting of the data in Figure 6.

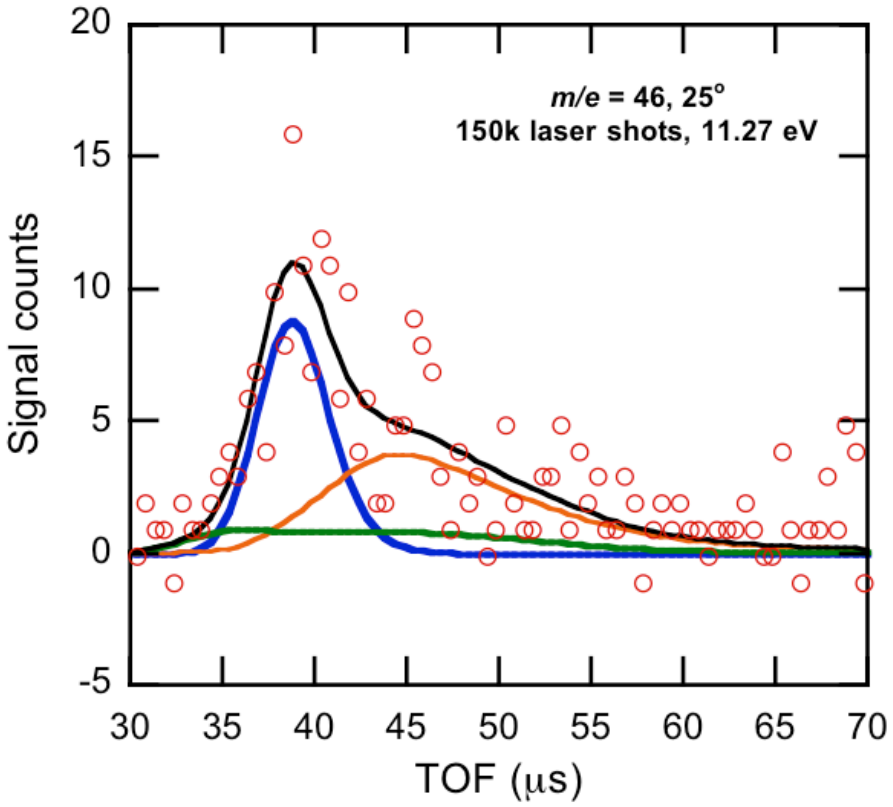

Figure 8: The TOF spectrum taken at m/e = 46 (CD_2CDO^+). The experimental data are shown in red open circles and the total fit is shown in black solid line. This total fit has several contributions, including dissociative ionization of stable CD_2CD_2OH radicals (blue) and the CD_2CDOH cofragment formed in the DBr photoelimination channel (orange). The remainder of the signal could be attributed to the dissociation of the neutral CD_2CD_2OH excited radicals to HD + vinoxy-d_3; the potential fit (green) was calculated using the secondary $P(E_T)$ given in Fig. 7 in this supplementary document.